Pair of accelerated black holes in a de Sitter background: the dS C-metric

Óscar J. C. Dias* and José P. S. Lemos†
Centro Multidisciplinar de Astrofísica - CENTRA,
Departamento de Física, Instituto Superior Técnico,
Av. Rovisco Pais 1, 1049-001 Lisboa, Portugal
(Dated: February 1, 2008)

Following the work of Kinnersley and Walker for flat spacetimes, we have analyzed the anti-de Sitter C-metric in a previous paper. In the de Sitter case, Podolský and Griffiths have established that the de Sitter C-metric (dS C-metric) found by Plebański and Demiański describes a pair of accelerated black holes in the dS background with the acceleration being provided (in addition to the cosmological constant) by a strut that pushes away the two black holes or, alternatively, by a string that pulls them. We extend their analysis mainly in four directions. First, we draw the Carter-Penrose diagrams of the massless uncharged dS C-metric, of the massive uncharged dS C-metric and of the massive charged dS C-metric. These diagrams allow us to clearly identify the presence of two dS black holes and to conclude that they cannot interact gravitationally. Second, we revisit the embedding of the dS C-metric in the 5D Minkowski spacetime and we represent the motion of the dS C-metric origin in the dS 4-hyperboloid as well as the localization of the strut. Third, we comment on the physical properties of the strut that connects the two black holes. Finally, we find the range of parameters that correspond to non-extreme black holes, extreme black holes, and naked particles.

PACS numbers: 04.20.Jb,04.70.Bw,04.20.Gz

arXiv:hep-th/0301046v2 13 May 2003

I. INTRODUCTION

In a previous paper [1] we have analyzed in detail the physical interpretation and properties of the anti-de Sitter C-metric, i.e., the C-metric with a negative cosmological constant, following the approach of Kinnersley and Walker [2] for the flat C-metric. We have concluded that it describes a pair of accelerated black holes when the acceleration A and the cosmological length ℓ are related by $A > 1/\ell$. The de Sitter C-metric (dS C-metric), i.e., the C-metric with a positive cosmological constant, was introduced by Plebański and Demiański [3], and its physical interpretation was first analyzed by Podolský and Griffiths [4]. A special case of it has been applied in the study of the quantum process of pair creation of black holes by Mann and Ross [5], and by Booth and Mann [6] (see [7] for a review). The dS C-metric describes a pair of accelerated black holes in the dS background with the acceleration being provided (in addition to the cosmological constant) by a strut that pushes away the two black holes or, alternatively, by a string that pulls them. In this paper, we are interested in further extend the physical interpretation of the de Sitter C-metric mainly in four directions. First, we draw the Carter-Penrose diagrams of the dS C-metric. These diagrams allow us to clearly identify the presence of two dS black holes and to conclude that they cannot interact gravitationally. Second, we revisit the embedding of the dS C-metric in the 5D Minkowski spacetime and we represent the motion of the dS C-metric origin in the dS 4-hyperboloid as well as the localization of the strut. Third, we discuss the physical properties of the strut that connects the two black holes. Finally, we find the range of parameters (cosmological constant, acceleration, mass and charge) that correspond to non-extreme black holes, extreme black holes, and naked particles.

The plan of this article is as follows. In section II we present the dS C-metric and analyze its curvature and conical singularities. In section III we study the causal diagrams of the solution. In section IV we give and justify a physical interpretation to the solution. The description of the solution in the dS 4-hyperboloid and the physics of the strut are analyzed. Finally, in section V concluding remarks are presented. For the comparison with the C-metric in the anti-de Sitter background, as well as for a fuller set of references on the C-metric, see [1].

II. GENERAL PROPERTIES

In this section, we will briefly mention some general properties of the dS C-metric that are well established. For details we ask the reader to see, e.g., [1, 2]. The dS C-metric, i.e., the C-metric with positive cosmological constant Λ, has been obtained by Plebański and Demiański [3]. For zero rotation and zero NUT parameter, the gravitational field of the dS C-metric is given by (see [1])

$$ds^2 = [A(x+y)]^{-2}(-\mathcal{F}dt^2 + \mathcal{F}^{-1}dy^2 + \mathcal{G}^{-1}dx^2 + \mathcal{G}dz^2)\,, \tag{1}$$

where

$$\mathcal{F}(y) = -\left(\frac{1}{\ell^2 A^2} + 1\right) + y^2 - 2mAy^3 + q^2A^2y^4,$$
$$\mathcal{G}(x) = 1 - x^2 - 2mAx^3 - q^2A^2x^4\,, \tag{2}$$

*Electronic address: oscar@fisica.ist.utl.pt
†Electronic address: lemos@kelvin.ist.utl.pt

and the non-zero components of the electromagnetic vector potential, $A_\mu dx^\mu$, are given by

$$A_{\rm t} = -e\, y\,, \qquad A_{\rm z} = g\, x\,. \tag{3}$$

This solution depends on four parameters namely, the cosmological length $\ell^2 \equiv 3/\Lambda$, $A > 0$ which is the acceleration of the black holes (see section IV), and m and q which are interpreted as the ADM mass and electromagnetic charge of the non-accelerated black holes, respectively (see Appendix). In general, $q^2 = e^2 + g^2$ with e and g being the electric and magnetic charges, respectively.

The coordinates used in Eqs. (1)-(3) hide the physical interpretation of the solution. To understand the physical properties of the solution we will introduce progressively new coordinates more suitable to this propose, following the approach of Kinnersley and Walker [2] and Ashtekar and Dray [8]. Although the alternative approach of Bonnor [9] simplifies in a way the interpretation, we cannot use it were since the cosmological constant prevents such a coordinate transformation into the Weyl form.

We start by defining a coordinate r as

$$r = [A(x+y)]^{-1}\,, \tag{4}$$

which is interpreted as a radial coordinate. Indeed, calculating a curvature invariant of the metric, namely the Kretschmann scalar,

$$R_{\mu\nu\alpha\beta}R^{\mu\nu\alpha\beta} = \frac{24}{\ell^2} + \frac{8}{r^8}\Big[6m^2r^2 + 12mq^2(2Axr-1)r + q^4(7 - 24Axr + 24A^2x^2r^2)\Big]\,, \tag{5}$$

we conclude that it is equal to $24/\ell^2$ when the mass m and charge q are both zero. Moreover, when at least one of these parameters is not zero, the curvature invariant diverges at $r = 0$, revealing the presence of a curvature singularity. Finally, when we take the limit $r \to \infty$, the curvature invariant approaches the expected value for a spacetime which is asymptotically dS.

We will consider only the values of Λ, A, m, and q for which $\mathcal{G}(x)$ has at least two real roots, $x_{\rm s}$ and $x_{\rm n}$ (say) and will demand that x belongs to the range $[x_{\rm s}, x_{\rm n}]$ where $\mathcal{G}(x) \geq 0$. By doing this we guarantee that the metric has the correct signature $(-+++)$ [see Eq. (1)] and that the angular surfaces Σ (t =const and r =const) are compact (see also the discussion in [10]). In these angular surfaces we now define two new coordinates,

$$\theta = \int_x^{x_{\rm n}} \mathcal{G}^{-1/2} dx\,, \qquad \phi \;=\; z/\kappa\,, \tag{6}$$

where ϕ ranges between $[0, 2\pi]$ and κ is an arbitrary positive constant which will be discussed soon. The coordinate θ ranges between the north pole, $\theta = \theta_{\rm n} = 0$, and the south pole, $\theta = \theta_{\rm s}$ (not necessarily at π). In general, if we draw a small circle around the north or south pole, as the radius goes to zero, the limit circunference/radius is not 2π. Indeed there is a deficit angle at the poles given by $\delta_{\rm n/s} = 2\pi[1 - (\kappa/2)|d_x\mathcal{G}|_{x_{\rm n/s}}]$. The value of κ can be chosen in order to avoid a conical singularity at one of the poles but we cannot remove simultaneously the conical singularities at both poles (for a more detailed analysis see [1]).

Rewritten in terms of the new coordinates introduced in Eq. (4) and Eq. (6), the dS C-metric is given by

$$ds^2 = r^2[-\mathcal{F}(y)dt^2 + \mathcal{F}^{-1}(y)dy^2 + d\theta^2 + \kappa^2\mathcal{G}(x_{(\theta)})d\phi^2]\,, \tag{7}$$

where $\mathcal{F}(y)$ and $\mathcal{G}(x_{(\theta)})$ are given by Eq. (2) and the time coordinate t can take any value from the interval $]-\infty, +\infty[$. When m or q are not zero there is a curvature singularity at $r = 0$. Therefore, we restrict the radial coordinate to the range $[0, +\infty[$. On the other hand, we have restricted x to belong to the range $[x_{\rm s}, x_{\rm n}]$ where $\mathcal{G}(x) \geq 0$. From $Ar = (x+y)^{-1}$ we then conclude that y must belong to the range $-x \leq y < +\infty$. Indeed, $y = -x$ corresponds to $r = +\infty$, and $y = +\infty$ to $r = 0$. Note however that when both m and q vanish there are no restrictions on the ranges of r and y (i.e., $-\infty < r < +\infty$ and $-\infty < y < +\infty$) since in this case there is no curvature singularity at the origin of r to justify the constraint on the coordinates.

III. CAUSAL STRUCTURE

In this section we analyze the causal structure of the solution. The original dS C-metric, Eq. (7), is not geodesically complete. To obtain the maximal analytic spacetime, i.e., to draw the Carter-Penrose diagrams we will introduce the usual null Kruskal coordinates. The description of the solution depends crucially on the values of m and q. We will consider the three most relevant solutions, namely: *A. Massless uncharged solution* ($m = 0$, $q = 0$), *B. Massive uncharged solution* ($m > 0$, $q = 0$), and *C. Massive charged solution* ($m \geq 0$, $q \neq 0$).

A. Massless uncharged solution ($m = 0, q = 0$)

In this case we have $x \in [x_{\rm s} = -1, x_{\rm n} = +1]$, $x = \cos\theta$, $\mathcal{G} = 1 - x^2 = \sin^2\theta$, $\kappa = 1$ and

$$\mathcal{F}(y) = y^2 - y_+^2 \qquad \text{with} \qquad y_+ = \sqrt{1 + \frac{1}{\ell^2 A^2}}\,. \tag{8}$$

The general behavior of these functions for this case is represented in Fig. 1.

The angular surfaces Σ (t =const and r =const) are spheres and both the north and south poles are free of conical singularities. The origin of the radial coordinate r has no curvature singularity and therefore both r and y can lie in the range $]-\infty, +\infty[$. However, in the realistic general case, where m or q are non-zero, there is

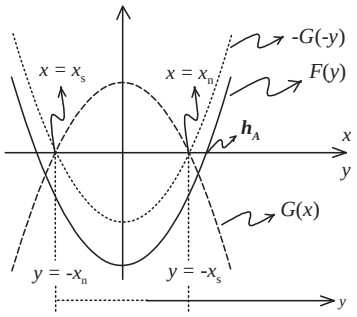

FIG. 1: Shape of $\mathcal{G}(x)$ and $\mathcal{F}(y)$ for the $m = 0, q = 0$ dS C-metric. The allowed range of x is between $x_{\rm s} = -1$ and $x_{\rm n} = +1$ where $\mathcal{G}(x)$ is positive and compact. The range of y is restricted to $-x \leq y < +\infty$. The presence of an accelerated horizon is indicated by h_A. It coincides with the cosmological horizon of the solution and has a non-spherical shape.

a curvature singularity at $r = 0$. Since the discussion of the present section is only a preliminary to that of the massive general case we will treat the origin $r = 0$ as if it had a curvature singularity and thus we admit that r belongs to the range $[0, +\infty[$ and y lies in the region $-x \leq y < +\infty$. We leave a discussion on the extension to negative values of r to section IV A.

To construct the Carter-Penrose diagram we first introduce the advanced and retarded Finkelstein-Eddington null coordinates,

$$u = t - y_* \,; \qquad v = t + y_* \,, \tag{9}$$

where the tortoise coordinate coordinate is

$$y_* = \int \mathcal{F}^{-1} dy = \frac{1}{2y_+} \ln \left| \frac{y - y_+}{y + y_+} \right| = \frac{1}{2}(v - u) \,. \tag{10}$$

and both u and v belong to the range $]-\infty, +\infty[$. In these coordinates the metric is given by

$$ds^2 = r^2[-\mathcal{F} du dv + d\theta^2 + \sin^2\theta \, d\phi^2] \,, \tag{11}$$

and his adjusted to the grid of null geodesics. Nevertheless, the metric still has the presence of a coordinate singularity at the root y_+ of $\mathcal{F}$. To overcome this undesirable situation we have to introduce the Kruskal coordinates. The demand that y must belong to the range $[-x; +\infty[$ implies that we have a region I, $-x \leq y < +y_+$, where $\mathcal{F}(y)$ is negative and a region II, $y_+ < y < +\infty$, where $\mathcal{F}(y)$ is positive (see Fig. 1). There is a Rindler-like acceleration horizon (r_A) at $y = y_+$. This acceleration horizon coincides with the cosmological horizon. In region I one sets the Kruskal coordinates $u' = +e^{-\lambda u}$ and $v' = +e^{+\lambda v}$ so that $u'v' = +e^{2\lambda y_*}$. In region II one defines $u' = -e^{-\lambda u}$ and $v' = +e^{+\lambda v}$ in order that $u'v' = -e^{2\lambda y_*}$. We set $\lambda \equiv y_+$. In both regions the product $u'v'$ is given by

$$u'v' = -\frac{y - y_+}{y + y_+} \,, \tag{12}$$

and the metric (11) expressed in terms of the Kruskal coordinates is given by

$$\begin{aligned} ds^2 &= r^2 \left[\frac{1}{y_+^2} \frac{\mathcal{F}}{u'v'} du' dv' + d\theta^2 + \sin^2\theta \, d\phi^2 \right] \\ &= r^2 \left[-\frac{(y + y_+)^2}{y_+^2} du' dv' + d\theta^2 + \sin^2\theta \, d\phi^2 \right] , \end{aligned} \tag{13}$$

with y and $Ar = (x + y)^{-1}$ regarded as functions of u' and v',

$$y = y_+ \frac{1 - u'v'}{1 + u'v'} \,, \quad Ar = \frac{1 + u'v'}{(y_+ + x) - u'v'(y_+ - x)} \,. \tag{14}$$

The Kruskal coordinates in both regions were chosen in order to obtain a negative value for the factor $\mathcal{F}/(u'v')$, which appears in the metric coefficient $g_{u'v'}$. The value of constant λ was selected in order that the limit of $\mathcal{F}/(u'v')$ as $y \to y_+$ stays finite and different from zero. By doing this, we have removed the coordinate singularity that was present at the root y_+ of $\mathcal{F}$ [see Eq. (11)]. So, the metric is now well-behaved in the whole range $-x \leq y < +\infty$ or $0 \leq r < +\infty$. At the edges of the interval allowed for r, the product $u'v'$ takes the values

$$\lim_{r \to 0} u'v' = -1 \,, \qquad \lim_{r \to +\infty} u'v' = \frac{y_+ + x}{y_+ - x} > 0 \text{ and finite} \,. \tag{15}$$

So, the original massless uncharged dS C-metric is described by the spacetime (13) subjected to the following coordinates ranges,

$$0 \leq \phi < 2\pi \,, \quad -1 \leq x \leq +1 \,, \quad u' < 0 \,, \quad v' > 0 \,, \tag{16}$$

$$-1 \leq u'v' < \frac{y_+ + x}{y_+ - x} \,. \tag{17}$$

This spacetime is however geodesically incomplete. To obtain the maximal analytical extension one allows the Kruskal coordinates to take also the values $u' \geq 0$ and $v' \leq 0$ as soon as the condition (17) is satisfied.

Finally, to construct the Carter-Penrose diagram one has to define the Carter-Penrose coordinates by the usual arc-tangent functions of u' and v': $\mathcal{U} = \arctan u'$ and $\mathcal{V} = \arctan v'$, that bring the points at infinity into a finite position. The Carter-Penrose diagram of the massless uncharged dS C-metric is sketched in Fig. 2. $r = 0$ is represented by a timelike line while $r = +\infty$ is a spacelike line (with $\mathcal{I}^-$ and $\mathcal{I}^+$ representing, respectively, the past and future infinity). The two mutual perpendicular straight null lines at 45°, $u'v' = 0$, represent a Rindler-like accelerated horizon.

To end this subsection it is important to remark that, contrary to what happens in the C-metric with $\Lambda < 0$ [1] and with $\Lambda = 0$ [2], the presence of the acceleration in the $\Lambda > 0$ C-metric does not introduce an extra horizon relatively to the $A = 0$ solution. Indeed, in the dS C-metric the acceleration horizon coincides with the cosmological

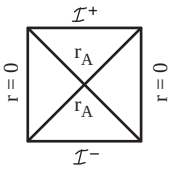

FIG. 2: Carter-Penrose diagram concerning the $m = 0, q = 0$ dS C-metric studied in section III A. The accelerated horizon is represented by r_A. It coincides with the cosmological horizon and has a non-spherical shape. $\mathcal{I}^-$ and $\mathcal{I}^+$ represent respectively the past and future infinity ($r = +\infty$). $r = 0$ corresponds to $y = +\infty$ and $r = +\infty$ corresponds to $y = -x$.

horizon that is already present in the $A = 0$ solution. However, in the $A = 0$ solution the cosmological horizon has the topology of a round sphere, while in the dS C-metric ($A \neq 0$) the presence of the acceleration induces a non-spherical shape in the acceleration (cosmological) horizon. This conclusion is set from the expression of the radius of the horizon, $r_A = A^{-1}(x + y_+)^{-1}$. It varies with the angular direction $x = \cos\theta$ and depends on the value of A [see Eq. (8)]. Another important difference between the causal structure of the dS C-metric and the causal structure of the $\Lambda = 0$ and the $\Lambda < 0$ cases is the fact that the general features of the Carter-Penrose diagram of the dS C-metric are independent of the angular coordinate $x = \cos\theta$. Indeed, in the $\Lambda < 0$ case [1] and in the $\Lambda = 0$ case [2], the Carter-Penrose diagram at the north pole direction is substantially different from the one along the south pole direction and different from the diagram along the equator direction (see [1, 2]).

B. Massive uncharged solution ($m > 0$, $q = 0$)

The construction of the Carter-Penrose diagram for the $m > 0$ dS C-metric follows up directly from the last subsection. We will consider the small mass or acceleration case, i.e., we require $27m^2A^2 < 1$ and we also demand x to belong to the range $[x_{\rm n}, x_{\rm s}]$ (represented in Fig. 3 and such that $x_{\rm s} \to -1$ and $x_{\rm n} \to +1$ when $mA \to 0$) where $\mathcal{G}(x) \geq 0$. By satisfying the two above conditions we endow the t =const and r =const surfaces Σ with the topology of a compact surface. For $27m^2A^2 \geq 1$ this surface is an open one and will not be discussed (see however [10]).

Now we turn our attention to the behavior of function $\mathcal{F}(y)$. We have to consider three distinct cases (see Fig. 4), namely: (i) pair of non-extreme dS-Schwarzschild black holes ($27m^2A^2 < 1 - 9m^2\Lambda$) for which $\mathcal{F}(y = 1/3mA) > 0$ (see Fig. 3), (ii) pair of extreme dS-Schwarzschild black holes ($27m^2A^2 = 1 - 9m^2\Lambda$) for which $\mathcal{F}(y = 1/3mA) = 0$, and (iii) case $27m^2A^2 > 1 - 9m^2\Lambda$ for which $\mathcal{F}(y)$ is always negative in the allowed range for y. This last case represents a naked particle and will not be discussed further. Notice that when we set $A = 0$ in the above relations we get the known results [11] for the non-accelerated dS spacetime, namely: for $9m^2\Lambda < 1$ we have the non-extreme dS-Schwarzschild solution and for $9m^2\Lambda = 1$ we get the extreme dS-Schwarzschild solution. In what follows we will draw the Carter-Penrose diagrams of cases (i) and (ii).

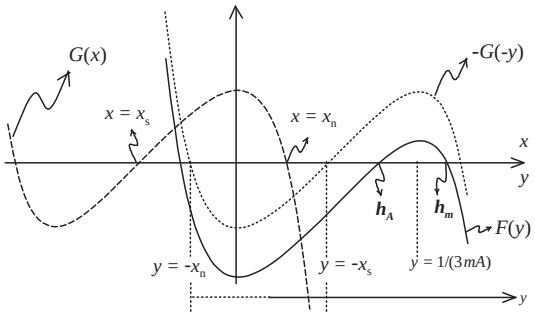

FIG. 3: Shape of $\mathcal{G}(x)$ and $\mathcal{F}(y)$ for the $27m^2A^2 < 1 - 9m^2\Lambda$, and $q = 0$ dS C-metric (case (i) in the text). The allowed range of x is between $x_{\rm s}$ and $x_{\rm n}$ where $\mathcal{G}(x)$ is positive and compact. The range of y is restricted to $-x \leq y < +\infty$. The presence of an accelerated horizon (which coincides with the cosmological horizon and has a non-spherical shape) is indicated by h_A and the Schwarzschild-like horizon by h_m. For completeness we comment on two other cases studied in the text: for $27m^2A^2 = 1 - 9m^2\Lambda$ (case (ii) in the text), $\mathcal{F}(y)$ is zero at its local maximum, i.e., h_A and h_m coincide. For $27m^2A^2 > 1 - 9m^2\Lambda$ (case (iii) in the text), $\mathcal{F}(y)$ is always negative in the allowed range of y.

(i) *Pair of non-extreme dS-Schwarzschild black holes* ($27m^2A^2 < 1 - 9m^2\Lambda$): the technical procedure to obtain the Carter-Penrose diagram is similar to the one described along section III A. In what concerns the physical conclusions, we will see that the essential difference is the presence of an extra horizon, a Schwarzschild-like horizon (r_+) due to the non-vanishing mass parameter, in addition to the accelerated Rindler-like horizon (r_A). Another important difference, as stated in section II, is the presence of a curvature singularity at the origin of the radial coordinate and the existence of a conical singularity at one of the poles. The Carter-Penrose diagram is drawn in Fig. 5.(i) and has a structure that can be divided into left, middle and right regions. The middle region contains the spacelike infinity (with $\mathcal{I}^-$ and $\mathcal{I}^+$ representing, respectively, the past and future infinity) and an accelerated Rindler-like horizon, $r_A = [A(x - x_-)]^{-1}$, that was already present in the $m = 0$ corresponding

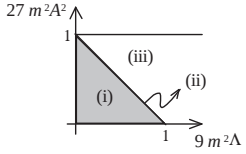

FIG. 4: Allowed ranges of the parameters Λ, A, and m for the cases (i), (ii), and (iii) of the uncharged massive dS C-metric discussed in the text of section III B.

(i) Non-extreme Black Hole

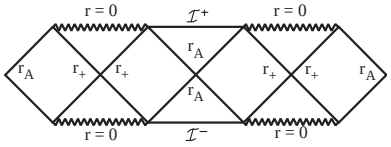

(ii) Extreme Black Hole

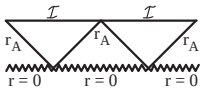

FIG. 5: (i) Carter-Penrose diagram of the $27m^2A^2 < 1 - 9m^2\Lambda$, and $q = 0$ dS C-metric discussed in case (i) of section III B. The zigzag line represents a curvature singularity, the accelerated horizon is represented by r_A. It coincides with the cosmological horizon and has a non-spherical shape. The Schwarzschild-like horizon is sketched as r_+. $r = 0$ corresponds to $y = +\infty$ and $r = +\infty$ ($\mathcal{I}^-$ and $\mathcal{I}^+$) corresponds to $y = -x$. (ii) Carter-Penrose diagram of the degenerate case (ii), $27m^2A^2 = 1 - 9m^2\Lambda$ and $q = 0$, discussed in the text of section III B. The accelerated horizon r_A coincides with the Schwarzschild-like horizon r_+.

diagram [see Fig. 2]. The left and right regions both contain a spacelike curvature singularity at $r = 0$ and a Schwarzschild-like horizon, r_+. This diagram is analogous to the one of the non-accelerated ($A = 0$) dS-Schwarzschild solution. However, in the $A = 0$ solution the cosmological and black hole horizons have the topology of a round sphere, while in the dS C-metric ($A \neq 0$) the presence of the acceleration induces a non-spherical shape in the acceleration horizon (that coincides with the cosmological horizon) and in the black hole horizon. Indeed, notice that once we find the zero, y_h, of $\mathcal{F}(y)$ that corresponds to an accelerated or black hole horizon, the position of these horizons depends on the angular coordinate x since $r_h = [A(x + y_h)]^{-1}$. In section IV B we will justify that this solution describes a pair of accelerated dS-Schwarzschild black holes.

(ii) *Pair of extreme dS-Schwarzschild black holes* ($27m^2A^2 = 1-9m^2\Lambda$): for this range of values, we have a degenerate case in which the size of the black hole horizon approaches and equals the size of the acceleration horizon. In this case, as we shall see in section IV B, the dS C-metric describes a pair of accelerated extreme dS-Schwarzschild black holes. The Carter-Penrose diagram of this solution is sketched in Fig. 5.(ii). It should be noted that for this sector of the solution, and as occurs with the $A = 0$ case, there is an appropriate limiting procedure [12] that takes this solution into the Nariai C-metric, i.e., the accelerated counterpart of the Nariai solution [13].

C. Massive charged solution ($m > 0$, $q \neq 0$)

When both the mass and charge parameters are non-zero, depending on the values of the parameters, $\mathcal{G}(x)$ can be positive in a single compact interval, $]x_{\rm s}, x_{\rm n}[$, or in two distinct compact intervals, $]x_{\rm s}, x_{\rm n}[$ and $]x'_{\rm s}, x'_{\rm n}[$, say. We require that x belongs to the interval $[x_{\rm s}, x_{\rm n}]$ (sketched in Fig. 6) for which the charged solutions are in the same sector of those we have analyzed in the last two subsections when $q \to 0$. Defining

$$\beta \equiv \frac{q^2}{m^2}\,, \quad 0 < \beta \leq \frac{9}{8}\,, \qquad \alpha_\pm \equiv 1 \pm \sqrt{1 - \frac{8}{9}\beta}\,,$$
$$\sigma(\beta, \alpha_\pm) = \frac{(4\beta)^2(3\alpha_\pm)^2 - 8\beta(3\alpha_\pm)^3 + \beta(3\alpha_\pm)^4}{(4\beta)^4}\,, \tag{18}$$

the above requirement is fulfilled by the parameter range $m^2A^2 < \sigma(\beta, \alpha_-)$. Now we look into the behavior of the function $\mathcal{F}(y)$. Depending on the sign of $\mathcal{F}(y)$ at $y_{\rm t}$ and $y_{\rm b}$ (with $y_{\rm t} = \frac{3\alpha_-}{4\beta mA}$ and $y_{\rm b} = \frac{3\alpha_+}{4\beta mA}$ being the points represented in Fig. 6 where the derivative of $\mathcal{F}(y)$ vanishes) we can group the solutions into five different relevant physical classes, namely: (i) $\mathcal{F}(y_{\rm t}) > 0$ and $\mathcal{F}(y_{\rm b}) < 0$, (ii) $\mathcal{F}(y_{\rm t}) > 0$ and $\mathcal{F}(y_{\rm b}) = 0$, (iii) $\mathcal{F}(y_{\rm t}) = 0$ and $\mathcal{F}(y_{\rm b}) < 0$, (iv) $\mathcal{F}(y_{\rm t}) > 0$ and $\mathcal{F}(y_{\rm b}) > 0$, and (v) $\mathcal{F}(y_{\rm t}) < 0$ and $\mathcal{F}(y_{\rm b}) < 0$. The ranges of parameters Λ, A, m, and β that correspond to these five cases are identified in Fig. 7. Condition $\mathcal{F}(y_{\rm t}) \geq 0$ requires $m^2A^2 \leq \sigma(\beta, \alpha_-) - m^2\Lambda/3$ and $\mathcal{F}(y_{\rm b}) \leq 0$ is satisfied by $m^2A^2 \geq \sigma(\beta, \alpha_+) - m^2\Lambda/3$. We have $\sigma(\beta, \alpha_-) > \sigma(\beta, \alpha_+)$ except at $\beta = 9/8$ where these two functions are equal; $\sigma(\beta, \alpha_-)$ is always positive; and $\sigma(\beta, \alpha_+) < 0$ for $0 < \beta < 1$ and $\sigma(\beta, \alpha_+) > 0$ for $1 < \beta \leq 9/8$. Case (i) has three horizons, the acceleration horizon h_A and the inner (h_-) and outer (h_+)

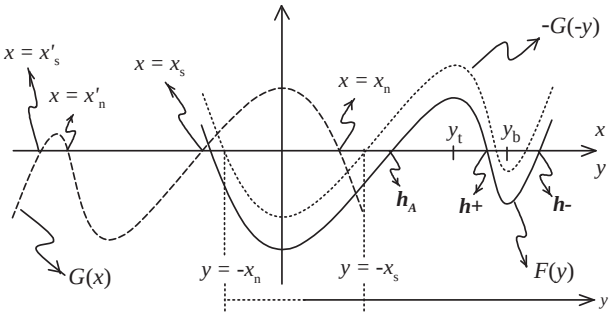

FIG. 6: Shape of $\mathcal{G}(x)$ and $\mathcal{F}(y)$ for the non-extreme charged massive dS C-metric (case (i) in the text of section III C). The allowed range of x is between $x_{\rm s}$ and $x_{\rm n}$ where $\mathcal{G}(x)$ is positive and compact. The presence of an accelerated horizon is indicated by h_A and the inner and outer charged horizons by $h-$ and $h+$. In the extreme cases, $h-$ and $h+$ [case (ii)] or $h-_A$ and $h+$ [case (iii)] superpose each other and in the naked case [case (iv) and (v)] $\mathcal{F}(y)$ has only one zero in the allowed range of y.

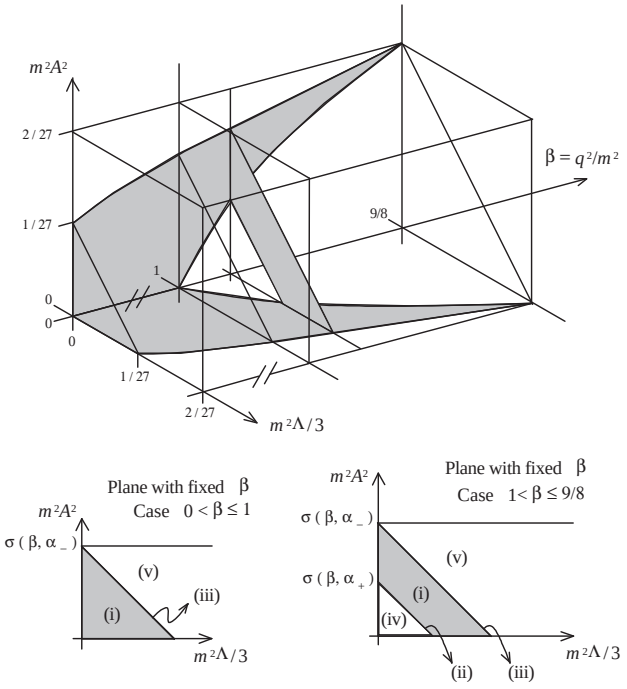

FIG. 7: Allowed ranges of the parameters $\Lambda, A, m, \beta \equiv q^2/m^2$ for the cases (i), (ii), (iii), (iv), and (v) of the charged massive dS C-metric discussed in the text of section III C.

charged horizons and is the one that is exactly represented in Fig. 6 ($h_A \neq h_+ \neq h_-$); in case (ii) the inner horizon and outer horizon coincide ($h_+ \equiv h_-$) and are located at $y_{\rm b}$ (h_A is also present); in case (iii) the acceleration horizon and outer horizon coincide ($h_A \equiv h_+$) and are located at $y_{\rm t}$ (h_- is also present); finally in cases (iv) and (v) there is a single horizon $h_A \equiv h_+ \equiv h_-$. As will be seen, case (i) describes a pair of accelerated dS−Reissner-Nordström (dS-RN) black holes, case (ii) describes a pair of extreme dS-RN black holes in which the inner and outer charged horizons become degenerated, case (iii) describes a pair of extreme dS-RN black holes in which acceleration horizon and outer charged horizon become degenerated, and cases (iv) and (v) describe a pair of naked charged particles. It should be noted that for the sector (iii) of the solution, and as occurs with the $A = 0$ case, there is an appropriate limiting procedure [12] that takes this solution into the charged Nariai C-metric, i.e., the accelerated counterpart of the charged Nariai solution [5, 13].

The essential differences between the Carter-Penrose diagram of the massive charged solutions and the diagram of the massive uncharged solutions are: (1) the curvature singularity is now represented by a timelike line rather than a spacelike line, (2) excluding the extreme and naked cases, there are now (in addition to the accelerated Rindler-like horizon, r_A) not one but two extra horizons, the expected inner (r_-) and outer (r_+) horizons associated to the charged character of the solution.

The Carter-Penrose diagram of case (i) is drawn in Fig. 8.(i) and has a structure that, as occurs in the massive uncharged case, can be divided into left, middle and right regions. The middle region contains the spacelike infinity and an accelerated Rindler-like horizon, r_A, that was already present in the $q = 0 = m$ corresponding diagram (see Fig. 2). The left and right regions both contain a timelike curvature singularity ($r = 0$), and an inner (r_-) and an outer (r_+) horizons associated to the charged character of the solution. This diagram is analogous the the one of the non-accelerated ($A = 0$) dS−Reissner-Nordström solution. However, in the $A = 0$ solution the cosmological and black hole horizons have the topology of a round sphere, while in the dS C-metric ($A \neq 0$) the presence of the acceleration induces a non-spherical

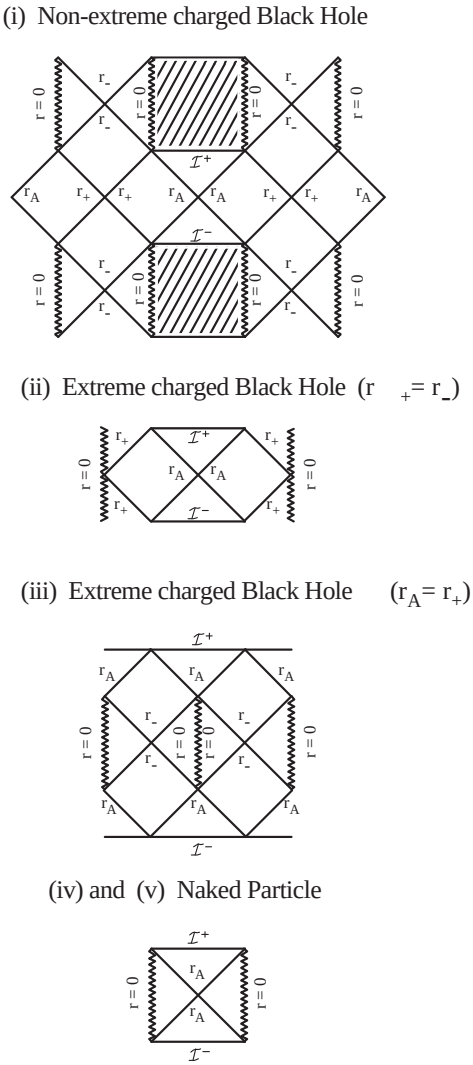

FIG. 8: Carter-Penrose diagrams of cases (i), (ii), (iii), and (iv) and (v) of the charged massive dS C-metric. The zigzag line represents a curvature singularity, an accelerated horizon is represented by r_A, the inner and outer charge associated horizons are sketched as r_- and r_+. $\mathcal{I}^-$ and $\mathcal{I}^+$ represent respectively the past and future infinity ($r = +\infty$). $r = 0$ corresponds to $y = +\infty$ and $r = +\infty$ corresponds to $y = -x$.

shape in the accelerated horizon (that coincides with the cosmological horizon) and in the black hole horizons. Indeed, notice that once we find the zero, y_h, of $\mathcal{F}(y)$ that corresponds to an accelerated or black hole horizon, the position of these horizons depends on the angular coordinate x since $r_h = [A(x + y_h)]^{-1}$. In Fig. 8 are also represented the other cases (ii)-(v). Again the accelerated horizon is in between two (extreme) black holes in cases (ii) and (iii) and in between two naked particles in cases (iv) and (v).

IV. PHYSICAL INTERPRETATION

The parameter A that is found in the dS C-metric is interpreted as being an acceleration and the dS C-metric describes a pair of black holes accelerating away from each other in a dS background. In this section we will justify this statement.

In the Appendix it is shown that, when $A = 0$, the general dS C-metric, Eq. (7), reduces to the dS ($m = 0\,,\, q = 0$), to the dS-Schwarzschild ($m > 0\,,\, q = 0$), and to the dS−Reissner-Nordström solutions ($m = 0\,,\, q \neq 0$). Therefore, the parameters m and q are, respectively, the ADM mass and ADM electromagnetic charge of the non-accelerated black holes. Moreover, if we set the mass and charge parameters equal to zero, even when $A \neq 0$, the Kretschmann scalar [see Eq. (5)] reduces to the value expected for the dS spacetime. This indicates that the massless uncharged dS C-metric is a dS spacetime in disguise.

In this section, we will first interpret case *A. Massless uncharged solution* ($m = 0,\ q = 0$), which is the simplest, and then with the acquired knowledge we interpret cases *B. Massive uncharged solution* ($m > 0,\ q = 0$) and *C. Massive charged solution* ($m > 0,\ q \neq 0$). We will interpret the solution following two complementary descriptions, the four dimensional (4D) one and the five dimensional (5D).

A. Description of the $m = 0$, $q = 0$ solution

The 4-Dimensional description:

As we said in III A, when $m = 0$ and $q = 0$ the origin of the radial coordinate r defined in Eq. (4) has no curvature singularity and therefore r has the range $]-\infty, +\infty[$. However, in the realistic general case, where m or q are non-zero, there is a curvature singularity at $r = 0$ and since the discussion of the massless uncharged solution was only a preliminary to that of the massive general case, following [8], we have treated the origin $r = 0$ as if it had a curvature singularity and thus we admitted that r belongs to the range $[0, +\infty[$. In these conditions we obtained the causal diagram of Fig. 2. Note however that one can make a further extension to include the negative values of r, enlarging in this way the range accessible to the Kruskal coordinates u' and v'. By doing this procedure we obtain the causal diagram of the dS spacetime, represented in Fig. 9.

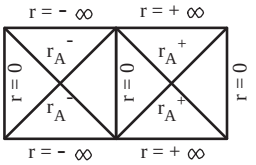

FIG. 9: Extending the Carter-Penrose diagram of Fig. 2 to negative values of r, we obtain the dS spacetime with its origin being accelerated. $r_A^- = [A(x - y_+)]^{-1} < 0$ and $r_A^+ = [A(x + y_+)]^{-1} > 0$.

Now, we want to clearly identify the parameter A that appears in the dS C-metric with the acceleration of its origin. To achieve this aim, we recover the massless uncharged dS C-metric defined by Eq. (1) and Eq. (2) (with $m = 0$ and $q = 0$), and after performing the following coordinate transformation [4]

$$\tau = \frac{\sqrt{1+\ell^2A^2}}{A}t\,, \qquad \rho = \frac{\sqrt{1+\ell^2A^2}}{A}\frac{1}{y}\,,$$
$$\theta = \arccos x\,, \qquad \phi = z\,, \tag{19}$$

we can rewrite the massless uncharged dS C-metric as

$$ds^2 = \frac{1}{\gamma^2}\left[-(1-\rho^2/\ell^2)d\tau^2 + \frac{d\rho^2}{1-\rho^2/\ell^2} + \rho^2 d\Omega^2\right], \tag{20}$$

with $d\Omega^2 = d\theta^2 + \sin^2\theta d\phi^2$ and

$$\gamma = \sqrt{1+\ell^2A^2} + A\rho\cos\theta\,. \tag{21}$$

At this point some remarks are convenient. The origin of the radial coordinate ρ corresponds to $y = +\infty$ and therefore to $r = 0$, where r has been introduced in Eq. (4). So, when we consider the massive dS C-metric there will be a curvature singularity at $\rho = 0$ (see section II). Moreover, when we set $A = 0$, Eq. (20) reduces to the usual dS spacetime written in static coordinates.

To discover the meaning of the parameter A we consider the 4D timelike worldlines described by an observer with $\rho =$const, $\theta = 0$ and $\phi = 0$ (see [4]). These are given by $x^\mu(\lambda) = (\gamma\ell\lambda/\sqrt{\ell^2-\rho^2}, \rho, 0, 0)$, were λ is the proper time of the observer and the 4-velocity $u^\mu = dx^\mu/d\lambda$ satisfies $u_\mu u^\mu = -1$. The 4-acceleration of these observers, $a^\mu = (\nabla_\nu u^\mu)u^\nu$, has a magnitude given by

$$|a_4| = \sqrt{a_\mu a^\mu} = \frac{\rho\sqrt{1+\ell^2A^2} + \ell^2 A}{\ell\sqrt{\ell^2-\rho^2}}\,. \tag{22}$$

Since $a_\mu u^\mu = 0$, the value $|a_4|$ is also the magnitude of the 3-acceleration in the rest frame of the observer. From Eq. (22) we achieve the important conclusion that the origin of the dS C-metric, $\rho = 0$ (or $r = 0$), is being accelerated with a constant acceleration $|a_4|$ whose value is

precisely given by the parameter A that appears in the dS C-metric. Moreover, at radius $\rho = \ell$ [or $y = y_+$ defined in equation (8)] the acceleration is infinite which corresponds to the trajectory of a null ray. Thus, observers held at ρ =const see this null ray as an acceleration horizon and they will never see events beyond this null ray. This acceleration horizon coincides with the dS cosmological horizon and has a non-spherical shape. For the benefit of comparison with the $A = 0$ dS spacetime, we note that when we set $A = 0$, Eq. (22) says that the origin, $\rho = 0$, has zero acceleration and at radius $\rho = \ell$ the acceleration is again infinite but now this is due only to the presence of the usual dS cosmological horizon which has a spherical shape.

The 5-Dimensional description:

In order to improve and clarify the physical aspects of the dS C-metric we turn now into the 5D representation of the solution.

The dS spacetime can be represented as the 4-hyperboloid,

$$-(z^0)^2 + (z^1)^2 + (z^2)^2 + (z^3)^2 + (z^4)^2 = \ell^2, \qquad (23)$$

in the 5D Minkowski embedding spacetime,

$$ds^2 = -(dz^0)^2 + (dz^1)^2 + (dz^2)^2 + (dz^3)^2 + (dz^4)^2. \qquad (24)$$

Now, the massless uncharged dS C-metric is a dS spacetime in disguise and therefore our next task is to understand how the dS C-metric can be described in this 5D picture. To do this we first recover the massless uncharged dS C-metric described by Eq. (20) and apply to it the coordinate transformation [4]

$$\begin{aligned} z^0 &= \gamma^{-1}\sqrt{\ell^2-\rho^2}\,\sinh(\tau/\ell)\,, \qquad z^2 = \gamma^{-1}\rho\sin\theta\cos\phi\,,\\ z^1 &= \gamma^{-1}\sqrt{\ell^2-\rho^2}\,\cosh(\tau/\ell)\,, \qquad z^3 = \gamma^{-1}\rho\sin\theta\sin\phi\,,\\ z^4 &= \gamma^{-1}[\sqrt{1+\ell^2A^2}\,\rho\cos\theta + \ell^2 A]\,, \end{aligned} \qquad (25)$$

where γ is defined in Eq. (21). Transformations (25) define an embedding of the massless uncharged dS C-metric into the 5D description of the dS spacetime since they satisfy Eq. (23) and take directly Eq. (20) into Eq. (24).

So, the massless uncharged dS C-metric is a dS spacetime, but we can extract more information from this 5D analysis. Indeed, let us analyze with some detail the properties of the origin of the radial coordinate, $\rho = 0$ (or $r = 0$). This origin moves in the 5D Minkowski embedding spacetime according to [see Eq. (25)]

$$\begin{aligned} &z^2 = 0\,,\ \ z^3 = 0\,,\ \ z^4 = \ell^2 A/\sqrt{1+\ell^2A^2} \ < \ell \quad \text{and}\\ &(z^1)^2 - (z^0)^2 = (A^2 + 1/\ell^2)^{-1} \equiv a_5^{-2}\,. \end{aligned} \qquad (26)$$

These equations define two hyperbolic lines lying on the dS hyperboloid which result from the intersection of this hyperboloid surface defined by Eq. (23) and the z^4=constant$< \ell$ plane (see Fig. 10). They tell us that the origin is subjected to a uniform 5D acceleration, a_5, and consequently moves along a hyperbolic worldline in the 5D embedding space, describing a Rindler-like motion (see Figs. 10 and 11) that resembles the well-known hyperbolic trajectory, $X^2 - T^2 = a^{-2}$, of an accelerated observer in Minkowski space. But uniformly accelerated radial worldlines in the 5D Minkowski embedding space are also uniformly accelerated worldlines in the 4D dS space [14], with the 5D acceleration a_5 being related to the associated 4D acceleration a_4 by $a_5^2 = a_4^2 + 1/\ell^2$. Comparing this last relation with Eq. (26) we conclude that $a_4 \equiv A$. Therefore, and once again, we conclude that the origin of the dS C-metric is uniformly accelerating with a 4D acceleration whose value is precisely given by the parameter A that appears in the dS C-metric, Eq. (1), and this solution describes a dS space whose origin is not at rest as usual but is being accelerated. For the benefit of comparison with the $A = 0$ dS spacetime, note that the origin of the $A = 0$ spacetime describes the hyperbolic lines $(z^1)^2 - (z^0)^2 = \ell^2$ which result from the intersection of the $z^4 = 0$ plane with the dS hyperboloid. In this case we can say that we have two antipodal points on the spatial 3-sphere of the dS space accelerating away from each other due only to the cosmological background acceleration. When $A \neq 0$ these two points suffer an extra acceleration. This discussion allowed us to find the physical interpretation of parameter A and to justify its label. Notice also that the original dS C-metric coordinates introduced in Eq. (1) cover only the half-space $z^1 > -z^0$. The Kruskal construction done in section III extended this solution to include also the $z^1 < -z^0$ region and so, in the extended solution, $r = 0$ is associated to two hyperbolas that represent two accelerated points (see Fig. 11). These two hyperbolas approach asymptotically the Rindler-like acceleration horizon (r_A).

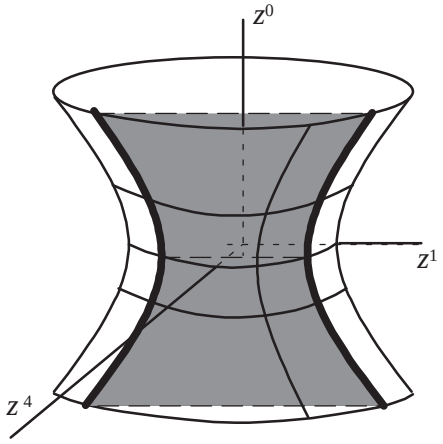

FIG. 10: The dS 4-hyperboloid embedded in the 5D Minkowski spacetime. The directions z^2 and z^3 are suppressed. The two hyperbolic lines lying on the dS hyperboloid result from the intersection of the hyperboloid surface with the z^4=constant$< \ell$ plane. They describe the motion of the origin of the dS C-metric ($A \neq 0$). For $A = 0$ the intersecting plane is $z^4 = 0$.

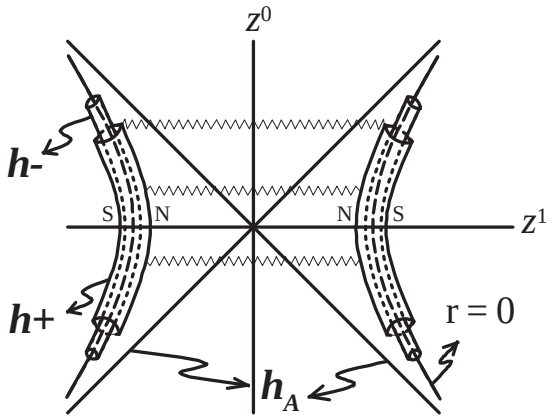

FIG. 11: Schematic diagram representing the 5D hyperbolic motion of two uniformly accelerating massive charged black holes approaching asymptotically the Rindler-like accelerated horizon (h_A). This horizon coincides with the cosmological horizon. The inner and outer charged horizons are represented by $h-$ and $h+$. The strut that connects the two black holes is represented by the zigzag lines. The north pole direction is represented by N and the south pole direction by S.

B. Pair of accelerated black holes ($m > 0$, $q \neq 0$)

Now, we are in a position to interpret the massive and charged solutions that describe two black holes accelerating away from each other. To see clearly this, let us look to the Carter-Penrose diagrams, Fig. 2, Fig. 5 and Fig. 8. Looking at these diagrams we can compare the different features that belong to the massless uncharge case (Fig. 2), to the non-extreme massive uncharged case [Fig. 5.(i)], and ending in the non-extreme massive charged case [Fig. 8).(i)]. In Fig. 2 we identify the two hyperbolas $r = 0$ (represented by two timelike lines) approaching asymptotically the Rindler-like acceleration horizon (r_A). When we add a mass to the solution we conclude that each of these two simple hyperbolas $r = 0$ are replaced by the more complex structure that represents a Schwarzschild black hole with its spacelike curvature singularity and its horizon [this is represented by r_+ in the left and right regions of Fig. 5.(i)]. So, the two accelerating points $r = 0$ have been replaced by two Schwarzschild black holes that approach asymptotically the Rindler-like acceleration horizon [represented by r_A in the middle region of Fig. 5.(i)]. The same interpretation can be assigned to the massive charged solution. The two hyperbolas $r = 0$ of Fig. 2 are replaced by two Reissner-Nordström black holes [with its timelike curvature singularity and its inner r_- and outer r_+ horizons; see the left and right regions of Fig. 8.(i)] that approach asymptotically the Rindler-like acceleration horizon already present in the $m = 0$ and $q = 0$ causal diagram. An issue that is relevant here, is whether the Cauchy horizons of the charged dS C-metric are stable. The Cauchy horizon of the non-accelerated dS−Reissner-Nordström black holes is stable to small perturbations, as shown in [15] (for a review on Cauchy horizon instabilities see, e.g., Burko and Ori [16]). Moreover, in [17] it has been shown that nearly extremal accelerating black holes in the flat background have stable Cauchy horizons, unlike the Cauchy horizon of the non-accelerated flat Reissner-Nordström black hole which is unstable. Therefore, we expect that the Cauchy horizons of the accelerated dS−Reissner-Nordström black holes are stable, although we do not have confirmed this result. The discussion of this subsection also applies directly to the extreme cases of the dS C-metric.

C. Source of acceleration and radiative properties

In this subsection we address the issue of the acceleration source and its localization. In the massless uncharged dS C-metric, observers that move along radial worldlines with ρ =const and $\theta = 0$ describe the Rindler-like hyperbola [see Eq. (25)]

$$(z^1)^2 - (z^0)^2 \;=\; \frac{\ell^2 - \rho^2}{(\sqrt{1+\ell^2 A^2} + A\rho)^2}\,. \qquad (27)$$

Moreover, when we put m or q different from zero, each of the two hyperbolas assigned to $r = 0$ represents the accelerated motion of a black hole. Thus, from Eq. (27) we conclude [1] that the north pole axis is in the region between the two black holes (see Fig. 11). Now, the value of the arbitrary parameter κ introduced in section II can be chosen in order to avoid a conical singularity at the south pole ($\delta_{\rm s} = 0$), leaving a conical singularity at the north pole ($\delta_{\rm n} < 0$). This is associated to a strut that joins the two black holes along their north poles and provides their acceleration [1]. This strut satisfies the relation $p = -\mu > 0$, where p and μ are respectively its pressure and its mass density [1]. Alternatively, we can choose κ such that avoids the deficit angle at the north pole ($\delta_{\rm n} = 0$) and leaves a conical singularity at the south pole ($\delta_{\rm s} > 0$). This option leads to the presence of a string (with $p = -\mu < 0$) that connects the two black holes along their south poles, and furnishes the acceleration.

The C-metric is an exact solution that emits gravitational and electromagnetic radiation. In the flat background the Bondi news functions have been explicitly calculated in [8, 18]. In dS background these calculations have not been carried yet, in fact dS still lacks a peeling theorem.

Ernst [19] has employed a Harrison-type transformation to the $\Lambda = 0$ charged C-metric in order to append a suitably chosen external electromagnetic field. With this procedure the so called Ernst solution is free of conical singularities at both poles and the acceleration that drives away the two oppositely charged Reissner-Nordström black holes is totally provided by the external

electromagnetic field. In the dS background we cannot remove the conical singularities through the application of the Harrison transformation [20]. Indeed, the Harrison transformation does not leave invariant the cosmological term in the action. Therefore, applying the Harrison transformation to Eqs. (1)-(3) does not yield a new solution of the Einstein-Maxwell-dS theory.

V. SUMMARY AND CONCLUSIONS

In a previous paper [1] we have analyzed in detail the physical interpretation and properties of the anti-de Sitter C-metric. In the dS background, Podolský and Griffiths [4] have established that the dS C-metric found by Plebański and Demiański [3] describes a pair of accelerated black holes with the acceleration being provided by a strut that connects the black holes together with the cosmological constant. We have extended their analysis essentially by drawing the Carter-Penrose diagrams of the solutions. These diagrams allowed us to clearly identify the presence of two dS black holes and to conclude that they cannot interact gravitationally. To obtain the physical interpretation of the solutions we have followed the approach of Kinnersly and Walker [2] for the flat C-metric. The alternative approach of Bonnor [9] which puts the flat C-metric into the Weyl form cannot be realized here, since the introduction of the cosmological constant prevents such a coordinate transformation.

The embedding of the massless uncharged dS C-metric into 5D Minkowski space clearly shows that the origin of the dS C-metric solution is subjected to a uniform acceleration, and describes a hyperbolic Rindler-like worldline in the dS 4-hyperboloid embedded in the 5D Minkowski space. To be more precise, the origin is represented by two hyperbolic lines that approach asymptotically the Rindler-like accelerated horizon. This acceleration horizon coincides with the cosmological horizon of the dS solution that is already present in the $A = 0$ solution. So, the presence of the extra acceleration caused by the strut does not introduce an extra horizon, contrary to what occurs in the the $\Lambda < 0$ C-metric [1] and in the $\Lambda = 0$ C-metric [2]. However, in the $A = 0$ dS solution the cosmological horizon has the topology of a round sphere, while in the dS C-metric ($A \neq 0$) the presence of the acceleration induces a non-spherical shape in the acceleration (cosmological) horizon.

When we add a mass or a charge to the system the causal diagrams indicate that now we have two dS-Schwarzschild or two dS−Reissner-Nordström black holes approaching asymptotically the Rindler-like accelerated horizon. The topology of all the horizons of these solutions is compact but non-spherical. In [4] the authors stated that since the origin of the massless uncharged dS C-metric corresponds to two accelerating points in de dS background then, when the mass and charge are small, the dS C-metric can be regarded as a perturbation of the massless uncharged dS C-metric. In this way they concluded that the dS C-metric describes a pair of accelerating black holes. With the Carter-Penrose diagrams of the massive and charged solutions, we have confirmed this result and we have found the range of parameters Λ, A, m, and q that correspond to non-extreme black holes, extreme black holes, and naked particles. The general features of the Carter-Penrose diagram of the dS C-metric are independent of the angular coordinate x. This sets a great difference between the causal diagrams of the dS C-metric and the ones of the $\Lambda < 0$ case [1] and of the $\Lambda = 0$ case [2]. Indeed, for the $\Lambda \leq 0$ C-metric, the Carter-Penrose diagram at the north pole direction is substantially different from the one along the south pole direction and different from the diagram along the equator direction (see [1, 2]).

We have proceeded to the localization of the conical singularity present in the solution. We have clearly identified the black hole north pole direction and shown that it points towards the other black hole. When the conical singularity is at the north pole, it is associated to a strut between the two black holes which satisfies the relation $p = -\mu > 0$, where p and μ are respectively the pressure on the strut and its mass density. The pressure is positive, so it points outwards and pulls the black holes apart, furnishing their acceleration (as in the flat and AdS C-metric). When the conical singularity is at the south pole, it is associated to a string between the two black holes with negative pressure that pushes the black holes away from each other.

The analysis of the Carter-Penrose diagrams of the dS C-metric has also been important to conclude that the two black holes cannot interact gravitationally. For example, looking into Fig. 5.(i) which represents the non-extreme massive uncharged C-metric we conclude that a null ray sent from the vicinity of one of the black holes can never cross the acceleration horizon (r_A) into the other black hole. Indeed, recall that in these diagrams the vertical axes represents the time flow and that light rays move along 45º lines. Thus, a light ray that is emitted from a region next to the horizon r_+ of the left black hole of Fig. 5.(i) can pass through the acceleration horizon r_A and, once it has done this, we will necessarily proceed into infinity $\mathcal{I}^+$. This light ray cannot enter the right region of Fig. 5.(i) and, in particular, it cannot hit the horizon r_+ of the right black hole. So, if the two black holes cannot communicate through a null ray they cannot interact gravitationally. The black holes accelerate away from each other only due to the pressure of the strut that connects the two black holes, in addition to the cosmological background acceleration contribution. This is coherent with the fact that there is no particular value of Λ and A for which the solution describes two black holes in a dS background whose relative distance remains fixed. Indeed, if the black holes could interact gravitationally then there would exist a particular set of parameter values for which the outward repulsion produced by the strut and by the cosmological constant would exactly cancel the inward gravitational attraction, and the

two black holes would be in equilibrium in the dS background. This is not the case precisely because the two black holes do not interact gravitationally. Note that the dS-Schwarzschild solution ($A = 0$) and the dS−Reissner-Nordström solution ($A = 0$) can be interpreted as a pair of gravitationally non-interacting black holes at antipodal points on the spatial 3-sphere of the dS space, which are accelerating away from each other due to the cosmological background acceleration. Similarly the massive and/or charged dS C-metric ($A \neq 0$) also describes a pair of gravitationally non-interacting black holes that accelerate away from each other in a dS background, but now they suffer an extra acceleration A provided by the strut or by the string that connects them.

Acknowledgments

This work was partially funded by Fundação para a Ciência e Tecnologia (FCT) through project CERN/FIS/43797/2001 and PESO/PRO/2000/4014. OJCD also acknowledges finantial support from FCT through PRAXIS XXI programme. JPSL thanks Observatório Nacional do Rio de Janeiro for hospitality.

APPENDIX: MASS AND CHARGE PARAMETERS

In this Appendix, one gives the physical interpretation of parameters m and q that appear in the dS C-metric. We follow [4]. Applying to Eq. (1) the coordinate transformations, $\tau = \sqrt{1+\ell^2A^2}A^{-1}t$, $\rho = \sqrt{1+\ell^2A^2}(Ay)^{-1}$, together with Eq. (6) and setting $A = 0$ (and $\kappa = 1$) one obtains

$$ds^2 = -F(\rho)\, d\tau^2 + F^{-1}(\rho)\, d\rho^2 + \rho^2(d\theta^2 + \sin^2\theta\, d\phi^2)\,, \tag{A.1}$$

where $F(\rho) = 1 - \rho^2/\ell^2 - 2m/\rho + q^2/\rho^2$. So, when the acceleration parameter vanishes, the dS C-metric, Eq. (1), reduces to the dS-Schwarzschild and dS−Reissner-Nordström black holes and the parameters m and q that are present in the dS C-metric are precisely the ADM mass and ADM electromagnetic charge of these non-accelerated black holes.

[1] O. J. C. Dias, J. P. S. Lemos, *Pair of accelerated black holes in anti-de Sitter background: the AdS C-metric*, Phys. Rev. D, in press; `hep-th/0210065`.

[2] W. Kinnersley, M. Walker, *Uniformly accelerating charged mass in General Relativity*, Phys. Rev. D **2**, 1359 (1970).

[3] J. F. Plebański, M. Demiański, *Rotating, charged and uniformly accelerating mass in general relativity*, Annals of Phys. **98**, 98 (1976).

[4] J. Podolský, J.B. Griffiths, *Uniformly accelerating black holes in a de Sitter universe*, Phys. Rev. D **63**, 024006 (2001).

[5] R. B. Mann, S. F. Ross, *Cosmological production of charged black hole pairs*, Phys. Rev. D **52**, 2254 (1995); R. B. Mann, *Charged topological black hole pair creation*, Nucl. Phys. B **516**, 357 (1998).

[6] I. S. Booth, R. B. Mann, *Cosmological pair production of charged and rotating black holes*, Nucl. Phys. B **539**, 267 (1999).

[7] O. J. C. Dias, *Pair creation of particles and black holes in external fields*, in *Astronomy and Astrophysics: Recent developments*, edited by J. P. S. Lemos et al (World Scientific, Singapore, 2001); `gr-qc/0106081`.

[8] A. Ashtekar, T. Dray, *On the existence of solutions to Einstein's equation with non-zero Bondi-news*, Comm. Phys. **79**, 581 (1981).

[9] W. B. Bonnor, *The sources of the vacuum C-metric*, Gen. Rel. Grav. **15**, 535 (1983).

[10] P. S. Letelier, S. R. Oliveira, *On uniformly accelerated black holes*, , Phys. Rev. D **64**, 064005 (2001).

[11] G. Gibbons, S. Hawking, *Cosmological event horizons, thermodynamics, and particle creation*, Phys. Rev. D **15**, 2738 (1977); K. Lake, R. Roeder, *Effects of a nonvanishing cosmological constant on the spherically symmetric vacuum manifold*, Phys. Rev. D **15**, 3513 (1977).

[12] O. J. C. Dias, J. P. S. Lemos, *The extremal limits of the C-metric: Nariai, Bertotti-Robinson and anti-Nariai C-metrics*, to be submitted (2003).

[13] H. Nariai, Science Reports of the Tohoku Univ. **35**, 62 (1951); P. Ginsparg, M. J. Perry, *Semiclassical perdurance of de Sitter space*, Nucl. Phys. B **222**, 245 (1983); S. W. Hawking, S. F. Ross, *Duality between electric and magnetic black holes*, Phys. Rev. D **52**, 5865 (1995); R. Bousso, *Adventures in de Sitter space*, `hep-th/0205177`.

[14] S. Deser, O. Levin, *Accelerated detectors and temperature in (anti-) de Sitter spaces*, Class. Quantum Grav. **14**, L163 (1997).

[15] F. Mellor, I. G. Moss, Phys. Rev. D **41**, 403 (1990); Class. Quantum Grav. **9**, L43 (1992); P. R. Brady, E. Poisson, Class. Quantum Grav. **9**, 121 (1992); P. R. Brady, D. Nunez, S. Sinha, Phys. Rev. D **47**, 4239 (1993).

[16] L. M. Burko, A. Ori, in *Internal structure of black holes and spacetime singularities*, edited by L. M. Burko and A. Ori (IOP, Bristol, 1997).

[17] G. T. Horowitz, H. J. Sheinblatt, Phys. Rev. D **55**, 650 (1997).

[18] J. Bičák, *Gravitational radiation from uniformly accelerated particles in general relativity*, Proc. Roy. Soc. A **302**, 201 (1968); V. Pravda, A. Pravdova, *Boost-rotation symmetric spacetimes - review*, Czech. J. Phys. **50**, 333 (2000); *On the spinning C-metric*, in *Gravitation: Following the Prague Inspiration*, edited by O. Semerák, J. Podolský, M. Zofka (World Scientific, Singapore, 2002), `gr-qc/0201025`.

[19] F. J. Ernst, *Removal of the nodal singularity of the C-metric*, J. Math. Phys. **17**, 515 (1976).

[20] R. Emparan, Private communication.